

PAPER • OPEN ACCESS

Study on Stress-strain Constitutive Relationship of Super-long-age Plastic Concrete under Triaxial Compression

To cite this article: Liangming Hu *et al* 2019 *IOP Conf. Ser.: Mater. Sci. Eng.* **585** 012018

View the [article online](#) for updates and enhancements.

Study on Stress-strain Constitutive Relationship of Super-long-age Plastic Concrete under Triaxial Compression

Liangming Hu^{1,a}, Junfu Zhu^{1,b,*}, Xin Jia^{1,c}, Changhui Zhang^{2,d}, Danying Gao^{1,e}

¹School of Water Conservancy and Environment Engineering, Zhengzhou University, Zhengzhou, 450001, China

²North China University of Water Resources and Electric Power, Zhengzhou, 450045, China

*Email: ^aliangmingh@zzu.edu.cn, ^b1537901727@qq.com, ^c420979646@qq.com, ^dzhangchanghui@ncwu.edu.cn, ^egdy@zzu.edu.cn

Abstract. The triaxial stress-strain relationship of super long-aged (540d) plastic concrete mixed with clay and bentonite was studied. According to the test, the stress-strain curves of plastic concrete under different confining pressures are obtained. It is found that the stress-strain curves under the lateral confining pressure are basically the same (0.4 MPa, 0.6 MPa), (0.4 MPa, 0.8 MPa), and the slope of the rising section is basically the same. Compared with the peak pressure ratio (0.2 MPa, 0.4 MPa), the lateral confining pressure is larger. In addition, the calculation formula of the peak secant elastic modulus and the triaxial compressive stress-strain relationship in accordance with the lateral pressure of plastic concrete are also proposed. The fourth-order polynomial mathematical model. The establishment of the mathematical model provides a basis for the development of plastic concrete specifications and triaxial compression performance numerical analysis, and further promotes the engineering application of plastic concrete.

1. Introduction

Plastic concrete is made by adding materials such as clay, bentonite, fly ash and other admixtures to concrete to enhance plasticity and reduce strength. Because of its good impermeability and deformation performance, in recent years, water conservancy and damming and Engineering and high-rise building foundation anti-seepage projects have been widely used [1–2]. In engineering applications, plastic concrete is usually in a three-dimensional compression state, and the principal stress values in three directions are different ($\sigma_1 \neq \sigma_2 \neq \sigma_3$). Due to the complex nature of the plastic concrete constituent materials, it is more realistic and reasonable to directly determine the multiaxial mechanical properties of the plastic concrete by the test method [3]. Therefore, it is necessary to carry out a triaxial test that reflects the true mechanical properties of concrete.

At present, most domestic scholars have carried out ordinary concrete triaxial tests [4–8], and research on plastic concrete is relatively rare. For plastic concrete, foreign expert Ahmad Mahboubi et al. conducted a triaxial compression test on plastic concrete. The study shows that the shear strength and cohesion of plastic concrete have a positive correlation with age, and the internal friction angle is opposite [9]; Nicholas et al. carried out an experimental study on the carbon fiber reinforced plastic concrete panels and established I-type fatigue model [10]; Hinchberger et al. Carried out experimental research and theoretical analysis on the basic mechanical properties of plastic concrete, the causes of crack formation, the calculation of crack depth, and the prevention of crack propagation [11–15]; And the International Dam Conference suggested that the elastic modulus of the plastic concrete should be



1~5 times of the elastic modulus of the surrounding soil [16]. The domestic Tsinghua University scholar Deng Mingji combined with the Dongping Lake anti-seepage project to study the uniaxial compression mechanical properties of clay plastic concrete and bentonite plastic concrete [17]; Domestic scholars Shi Yan and others studied the mechanical and triaxial stress-strain relationship of plastic concrete with low liquid limit clay, and found that the strength of plastic concrete decreases with the increase of clay content [18]; Song Shuaiqi et al studied The mechanical and impermeability properties of ash-plastic concrete in cement kiln [19]; Liu Lulu et al studied the stress-strain characteristics of plastic concrete under cyclic loading and unloading [20].

In general, there are few true triaxial compression tests for plastic concrete. In this paper, the constitutive relationship of super-long-age plastic concrete mixed with clay and bentonite under triaxial compression is studied, and the triaxial compression constitutive relation is established. The fourth-order polynomial mathematical model has important theoretical significance and practical application value for the study of plastic concrete.

2. Experimental Procedure

2.1. Test raw Materials

The experiment uses 42.5 # ordinary portland cement, calcium bentonite produced in Pingqiao Henan Xinyang, silty clay in the lake area of Longzi lake in Zhengdong new district, Zhengzhou city. The silty clay is retrieved and dried and ground to powder at a standard of 350 particle size. All the above indicators are in accordance with Ordinary Portland Cement (GB175-2007) [21]. The coarse aggregate used in the test is crushed stone with particle size of 5 ~ 20mm. The fine aggregate is natural river sand, and the fineness modulus is 2.7. It belongs to medium sand and the grading curve is in the second zone. The aggregates meet the requirements of Sand for Construction (GB/T14684 - 2011)[22] and Specifications for Hydraulic Concrete Construction (DL/T5144 - 2001)[23] standards.

2.2. Design Scheme of Mix Proportions of Plastic Concrete

In this experiment, clay and bentonite were used to replace part of the cement, and clay-bentonite-cement plastic concrete was made. The mass ratio method was used to design the mixture ratio. The sand ratio, water-to-binder ratio and unit water consumption were the three clear parameters in this test. The sand ratio is the ratio of the mass between sand and the total sand; the water-to-binder ratio is an indicator reflecting the ratio of the quality of water to cementitious materials (cement, bentonite and clay); the unit water consumption is the quality of the cement slurry and aggregate. After the trial distribution, the specific mix design was determined, as shown in Table 1.

Table 1. Mix proportions

Number	Water binder ratio	Sand ratio	Water /kg	Cement content / kg	Clay / kg	Bentonite /kg	Sand /kg	Cobblestone / kg
WB075	0.75	0.50	307.50	150	180	80	666.25	666.25
WB087	0.87	0.50	356.70	150	180	80	641.65	641.65
WB100	1.00	0.50	400	150	180	70	625	625
S04	1.00	0.40	370	120	180	70	524	786
S05	1.00	0.50	370	120	180	70	655	655
S06	1.00	0.60	370	120	180	70	786	524
CL180	0.87	0.50	322	120	180	70	655	655
CL220	0.87	0.50	357	120	220	70	641.5	641.5
CL260	0.87	0.50	391	120	260	70	604.5	604.5
B40	0.87	0.50	296	120	180	40	707	707
B70	0.87	0.50	322	120	180	70	655	655
B100	0.87	0.50	348	120	180	100	651	651

*WB: water binder ratio, S: sand ratio, CL: clay, B: Bentonite.

2.3. Experimental Method

According to the mixing ratio set in Table 1, 12 sets of 150mm × 150mm × 150mm plastic concrete cube specimens were prepared, and the specimens were cured 540d under standard curing conditions after pouring. This test uses a LY-C tensile true triaxial test for triaxial compression test. The test scheme is a triaxial compression test with a side pressure fixed. The triaxial compressive failure test is to apply a three-way pressure. The direction of σ_1 and σ_2 is increased to a predetermined confining pressure value, and the pressure is continuously applied to the concrete test in the direction of σ_3 . Piece of damage, triaxial compressive strength is the peak of the stress-strain curve in the σ_3 direction. In this test, combined with engineering experience, three confining pressure conditions were established, namely (1) $\sigma_1 = 0.2\text{MPa}$, $\sigma_2 = 0.4\text{MPa}$; (2) $\sigma_1 = 0.4\text{MPa}$, $\sigma_2 = 0.6\text{MPa}$; (3) $\sigma_1 = 0.4\text{MPa}$, $\sigma_2 = 0.8\text{MPa}$. Let $q = 1.0\text{MPa}$, simplified to (0.2q, 0.4q), (0.4q, 0.6q), (0.4q, 0.8q).

3. Test Results and Analysis

3.1. Triaxial Compressive Strength and Stress-strain Curve Characteristics of Plastic Concrete

The results of the triaxial compression test of the test piece and the typical stress-strain curves under different confining pressures are shown in Table 2 and Figure 1.

Table 2. Plastic concrete triaxial compressive strength

Number	triaxial compressive strength / MPa		
	(0.2q, 0.4q)	(0.4q, 0.6q)	(0.4q, 0.8q)
WB075	12.18	13.73	13.50
WB087	10.41	10.46	10.85
WB100	8.97	8.79	8.72
S04	7.38	7.49	7.54
S05	6.07	7.32	7.71
S06	7.90	8.43	8.54
CL180	8.63	10.16	10.57
CL220	9.04	9.82	10.40
CL260	6.50	7.59	6.93
B40	9.93	11.37	8.87
B70	8.63	10.16	10.57
B100	8.25	9.54	10.07

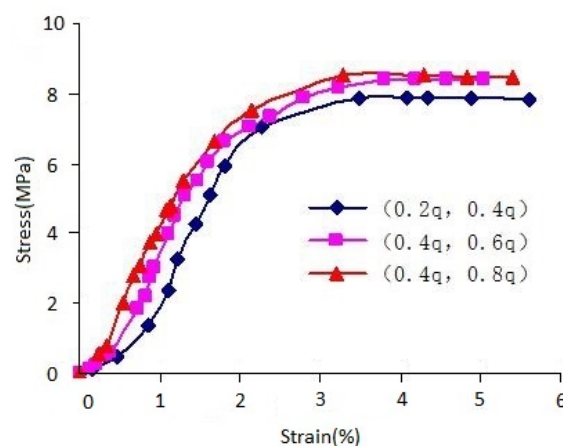


Figure 1. Stress-strain curves of plastic concrete under triaxial compression with constant lateral pressure

It can be seen from Table 2 that the plastic concrete triaxial compressive strengths with different mixing ratios are relatively different, and different confining pressure conditions have little effect on the concrete strength. It can be seen from Figure 1 that the three-axis compressive stress-strain curve under the condition of constant lateral pressure can be divided into two sections, namely the curve rising section and the horizontal section. When the three-way pressure is applied, the deformation of the specimen increases rapidly. However, as the pressure continues to increase, the principal stress gradually increases, and the lateral compressive stress constrains the lateral deformation of the plastic concrete. The generation and extension of cracks are delayed by the lateral constraint, the growth of the main strain becomes relatively slow, and the slope of the stress-strain curve increases. When the principal stress gradually increases to a large stress value, the plasticity of the plastic concrete specimen at this time the deformation begins to develop gradually, the strain increases rapidly, and the stress growth is slow. The corresponding stress-strain curve rises gently and the slope gradually decreases. When the stress-strain curve reaches the peak point, the test piece reaches the triaxial compressive strength and stress. It remains basically stable, the strain continues to increase, the stress-strain curve enters the horizontal section, and the principal stress σ_3 maintains the triaxial compressive strength.

3.2. Mathematical Model of Constitutive Relation of Plastic Concrete under Triaxial Compression

Plastic concrete is a nonlinear system composed of a variety of materials. If the linear elastic constitutive relation is used to describe the stress-strain relationship of plastic concrete, there is a large error. The mathematical model of the non-elastic constitutive equation is complex and involves many parameters. The process of derivation is quite cumbersome and is not conducive to popularization. Therefore, this paper proposes a mathematical model of the fourth-order polynomial form that conforms to the characteristics of the triaxial compression stress-strain curve of plastic concrete compression stress-strain curve is proposed.

3.2.1 The Relationship between the Peak Secant Modulus and the Peak Stress. It has been found that the elastic modulus of concrete increases with the increase of strength, showing a positive correlation, but the dispersion is large. In this paper, by analyzing the results of plastic concrete triaxial compression test, the formula for calculating the peak secant modulus and peak stress of plastic concrete is obtained, see equation (1).

$$E_f = a_1 \sigma_{3f} - a_2 \quad (1)$$

where $a_1 = 32.075\sigma_1 - 37.746 \frac{\sigma_1}{\sigma_n} + 55.522$, $a_2 = -333.45\sigma_1 + 387.36 \frac{\sigma_1}{\sigma_n} - 253.19$, E_f is the peak elastic modulus of plastic concrete under fixed lateral pressure, σ_{3f} is the triaxial compressive strength of plastic concrete, σ_1 , σ_2 are lateral compressive stress of plastic concrete.

According to the empirical equation of uniaxial compression modulus proposed by the American Standard (ACI318-08) and the former Soviet Union specification and the Chinese standard (GB50010-2002), the plastic concrete test data were fitted based on the stress-strain curve equation of concrete under uniaxial compression. The empirical equation for the elastic modulus of the peak secant of the plastic concrete under fixed lateral pressure is obtained as:

According to the American Standard (ACI318-08) and China Code (GB50010-2002) recommended uniaxial compression elastic modulus empirical calculation formula to fit the test data of plastic concrete, The empirical calculation formula for the elastic modulus and peak stress of the peak secant under the lateral compression of plastic concrete is expressed by equations (2) and (3):

$$E_f = b_1 \sqrt{\sigma_{3f}} + b_2 \quad (2)$$

Where $b_1 = 302.7\sigma_1 - 199.8 \frac{\sigma_1}{\sigma_n} + 283.69$, $b_2 = -947.25\sigma_1 + 641.04 \frac{\sigma_1}{\sigma_n} - 600.03$.

$$E_f = \frac{10^5}{c_1 + \frac{c_2}{\sigma_{3f}}} \quad (3)$$

Where $c_1 = 17426.5\sigma_1 - 10747.2\frac{\sigma_1}{\sigma_2} + 4817.2$, $c_2 = -1913.15\sigma_1 + 910.32\frac{\sigma_1}{\sigma_2} + 40.52$.

By comparing and analyzing the difference between the calculated value and the experimental value of formula (1), formula (2) and formula (3), Obtain the total average, mean square error and coefficient of variation of the ratio of the calculated values of the formulas to the experimental values, see Table 3. It can be found from Table 3 that the total mean value of the calculated value and the experimental value obtained by the formula (3) is 0.9992, the error is 0.08%, and the errors of the formula (1) and the formula (2) are 6.04% and 6.24%, respectively. In addition, the mean square error and coefficient of variation of the formula (3) are also the smallest, which can perfectly reflect the relationship between the peak secant elastic modulus and the peak stress. It is recommended to use the formula (3) as the calculation formula of the peak secant modulus.

Table 3. The comparison between calculated values of elastic modulus and experimental values

Equation number	Ratio of calculated values of elastic modulus to experimental ones		
	Average value	Mean square deviation	Coefficient of variation
(1)	1.0604	0.2787	0.2628
(2)	1.0624	0.2841	0.2675
(3)	0.9992	0.2437	0.2439

3.2.2 Mathematical model of constitutive relation of plastic concrete under triaxial compression. The stress-strain curve of the plastic concrete is fitted by the theoretical mathematical model. It is found that the quartic polynomial model agrees well with the measured curve. Therefore, the quartic polynomial mathematical model of stress-strain relation of plastic concrete under triaxial compression is put forward in this paper. That is:

$$y = Ax^4 + Bx^3 + Cx^2 + Dx \quad (x \leq 1) \quad (4)$$

$$y = 1 \quad (x > 1) \quad (5)$$

Where vertical and horizontal coordinates are $y = \sigma_3/\sigma_{3f}$, $x = \varepsilon_3/\varepsilon_{3f}$. ε_{3f} is the peak compressive strain corresponding to σ_{3f} .

When $\varepsilon_3 = \varepsilon_{3f}$, $\sigma_3 = \sigma_{3f}$, that is, $x = 1$, $y = 1$. Substituting $x = 1$ and $y = 1$ into Eq. (4) yields:

$$A + B + C + D = 1 \quad (6)$$

Both sides of the Eq. (4) make a derivative of ε_3 , then:

$$\frac{dy}{d\varepsilon_3} = (4Ax^3 + 3Bx^2 + 2Cx + D) \frac{dx}{d\varepsilon_3}$$

$$\frac{1}{\sigma_{3f}} \frac{d\sigma_3}{d\varepsilon_3} = (4Ax^3 + 3Bx^2 + 2Cx + D) \frac{1}{\varepsilon_{3f}}$$

Substituting $\varepsilon_3 = 0$, that is, $x=0$ into the equation:

$$\left. \frac{d\sigma_3}{d\varepsilon_3} \right|_{\varepsilon_3=0} = \frac{\sigma_{3f}}{\varepsilon_{3f}} D$$

$$D = \frac{E_0'}{E_f} \quad (7)$$

Where E_0' is initial tangential elastic modulus of plastic concrete under triaxial compression and $E_0' = \left. \frac{d\sigma_3}{d\varepsilon_3} \right|_{\varepsilon_3=0}$.

It can be seen from Eq. (7) that the model coefficients D are related to E_o'/E_f . Similarly, there is a close relationship between the model coefficients A, B, C and E_o'/E_f . The initial tangential elastic modulus E_o' is difficult to measure in the statistical analysis, so the measured uniaxial elastic modulus E_o is used instead of E_o' . E_f is calculated using Eq. (3). The curve equation of each specimen can be obtained by fitting based on the measured stress-strain curves, resulting in 33 values of A, B, C, D. And then these values are fitted to get equations of A, B, C, D as follows:

$$A = -0.1756\left(\frac{E_o}{E_f}\right)^2 + 1.6224\frac{E_o}{E_f} - 0.1773 \quad (8)$$

$$B = 0.1583\left(\frac{E_o}{E_f}\right)^2 - 1.0175\frac{E_o}{E_f} - 7.0733 \quad (9)$$

$$C = 0.1237\left(\frac{E_o}{E_f}\right)^2 - 1.8488\frac{E_o}{E_f} + 11.294 \quad (10)$$

$$D = -0.1064\left(\frac{E_o}{E_f}\right)^2 + 1.2452\frac{E_o}{E_f} - 3.0482 \quad (11)$$

E_o is the uniaxial compressive elastic modulus of plastic concrete with 90d age.

3.3. Verify the Fourth-order Polynomial Mathematical Model

In order to verify the reliability of the mathematical model established, the experimental measured curves of the test pieces of each group are compared with the theoretical model curves obtained by using equations (4) and (5), as shown in Fig. 2 to Fig. 12. From the comparison of the theoretical model curve and the experimental measured curve in Figure 2 to Figure 12, it can be seen that the theoretical model curve under the lateral confining pressure of (0.4q, 0.6q) almost coincides with the measured curve, (0.2q, 0.4q), (0.4q, 0.8q) There is a slight deviation between the theoretical curve and the measured curve under the lateral confining pressure, but the overall consistency is consistent, which fully proves that the established polynomial mathematical model has good reliability.

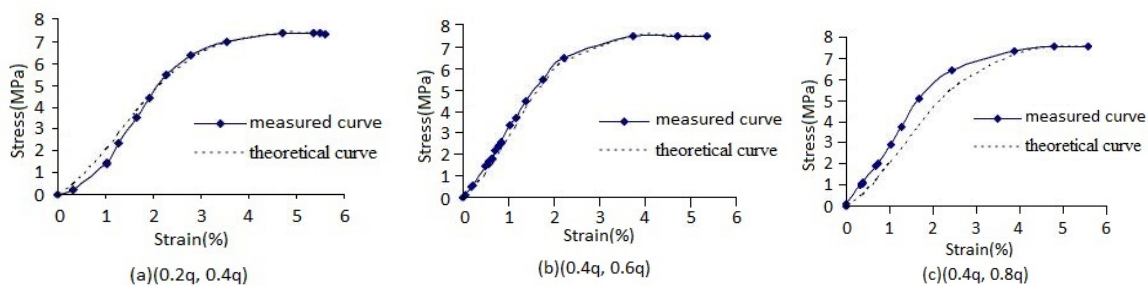


Figure 2. The comparison between theoretical curves and measured curves of S04 models

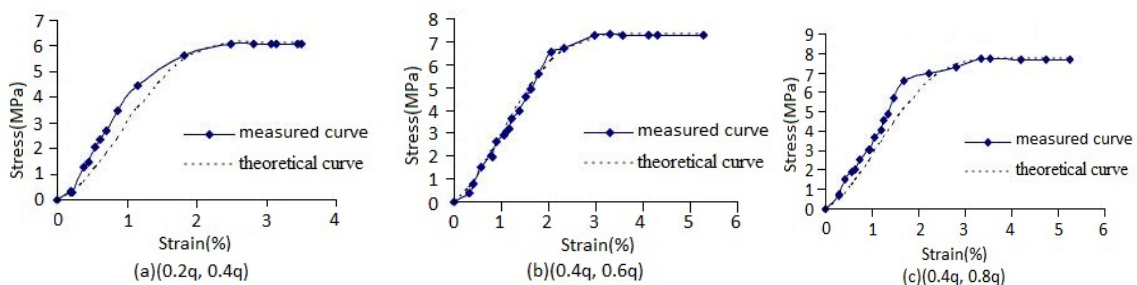


Figure 3. The comparison between theoretical curves and measured curves of S05 models

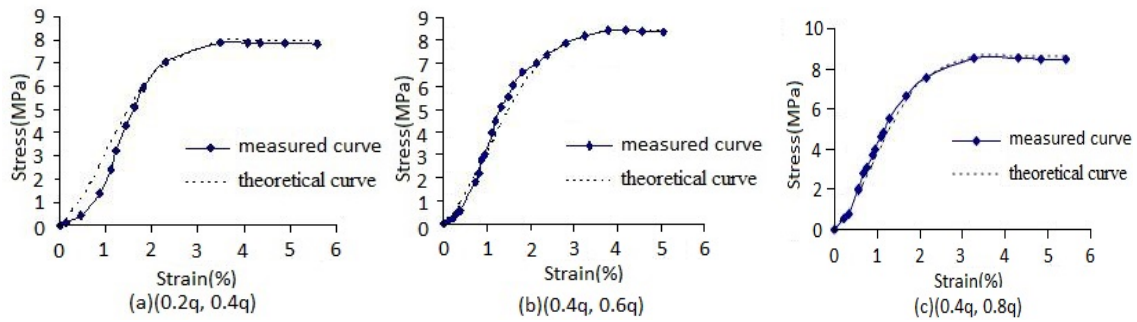


Figure 4. The comparison between theoretical curves and measured curves of S06 models

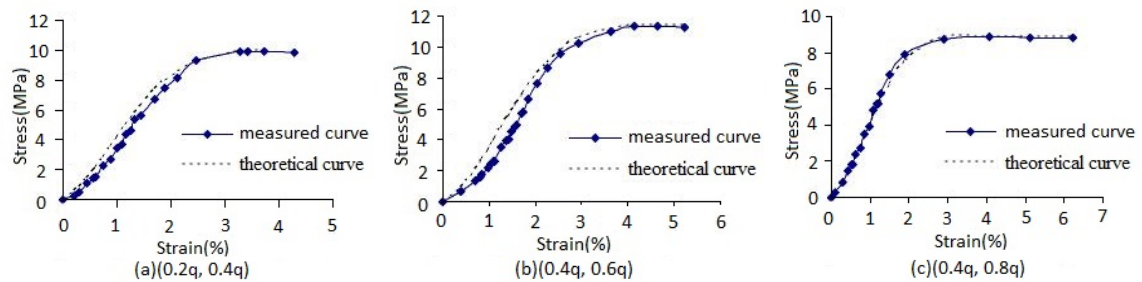


Figure 5. The comparison between theoretical curves and measured curves of B40 models

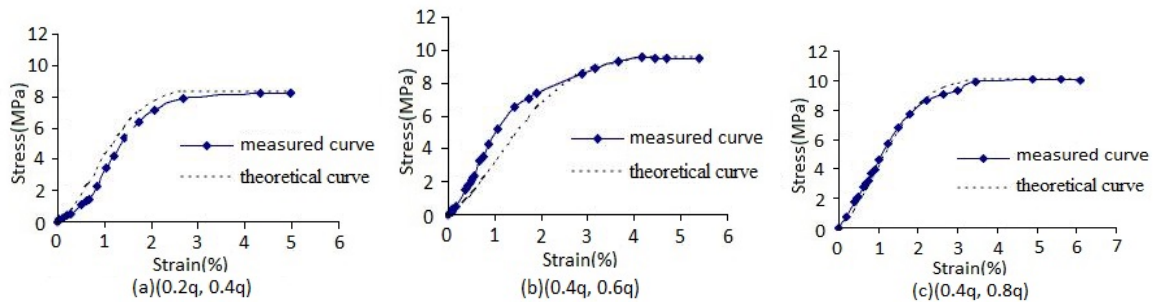


Figure 6. The comparison between theoretical curves and measured curves of B100 models

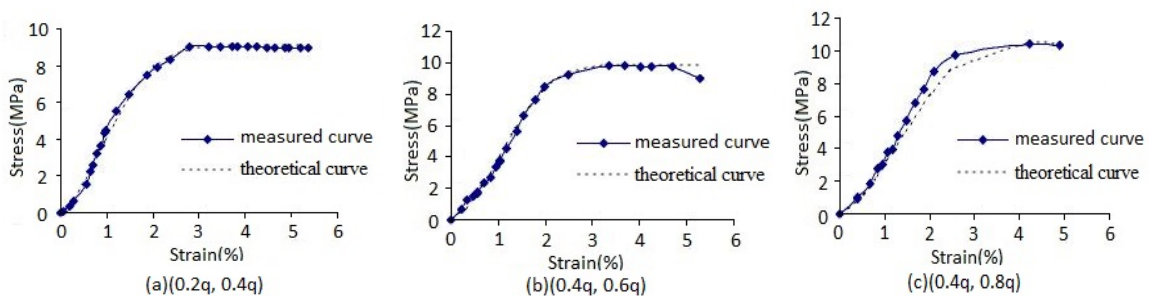


Figure 7. The comparison between theoretical curves and measured curves of CL220 models

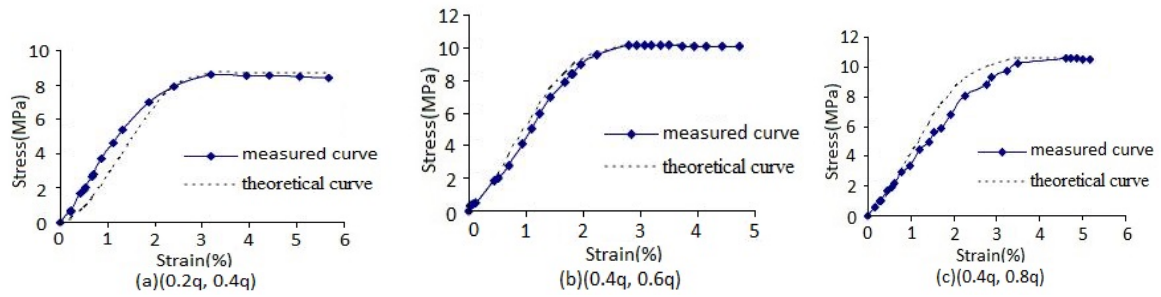


Figure 8. The comparison between theoretical curves and measured curves of CL180, B70 models

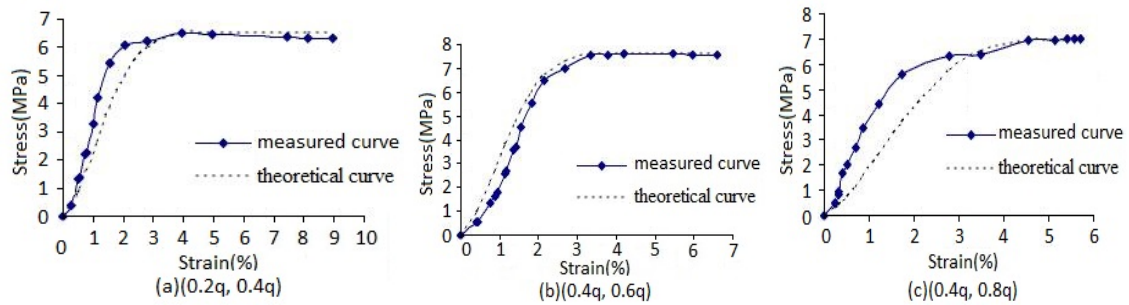


Figure 9. The comparison between theoretical curves and measured curves of CL260 models

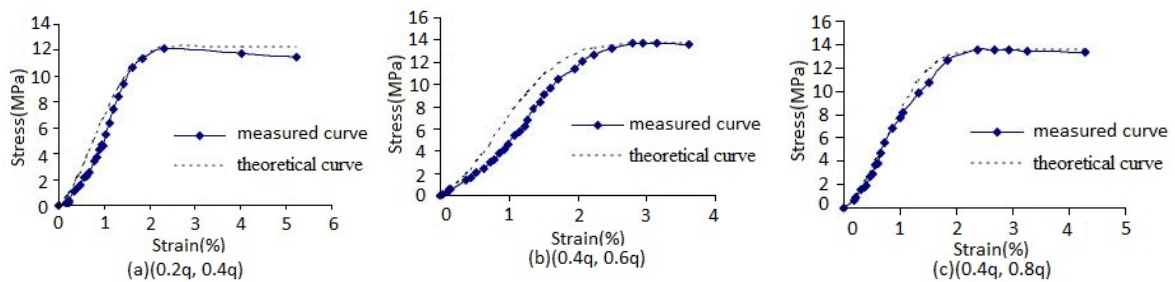


Figure 10. The comparison between theoretical curves and measured curves of WB075 models

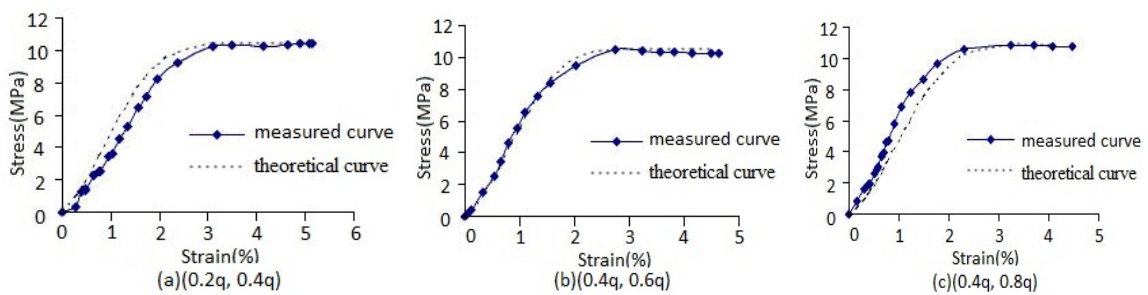


Figure 11. The comparison between theoretical curves and measured curves of WB087 models

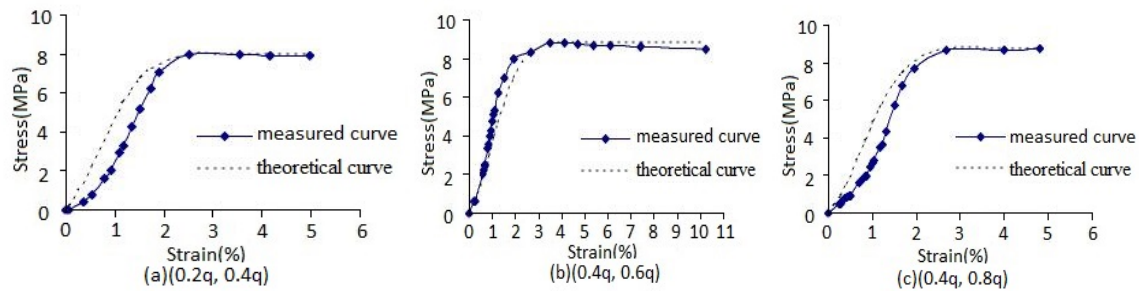


Figure 12. The comparison between theoretical curves and measured curves of WB100 models

4. Conclusions

1. The slope of the 540 d plastic concrete in the rising section of the stress-strain curve under the medium-high lateral confining pressure is larger than the low confining pressure, but the compressive strength is not much different.

2. Refer to different specifications to obtain the calculation formula of the compressive peak secant modulus of plastic concrete. After comparison, it is recommended that the triaxial compression peak secant modulus be calculated by formula (3).

3. A quadratic polynomial mathematical model conforming to the triaxial compression constitutive relation of plastic concrete is fitted, and the model has good reliability.

5. Acknowledgments

This work was supported by National Natural Science Foundation of China (Project No. 50979100). The study received helpful assistance from College of water resources and environment, Zhengzhou University, and North China University of Water Resources and Electric Power.

6. References

- [1] LM. Hu, Stress-strain relation model and failure criterion of plastic concrete under compression, Doc. Diss. of Zhengzhou Univ. (2012). (in Chinese)
- [2] DY. Gao, SQ. Song, Performance and failure criteria for plastic concrete under biaxial compressive stress. *J. Hydraul. Eng.* 47(1) (2016) 10-17. (in Chinese)
- [3] DY. Gao, SQ. Song, L. Yang, Performance and failure criteria for plastic concrete under true tri-axial compressive stress. *J. Hydraul. Eng.* 45(3) (2014) 360-367. (in Chinese)
- [4] JW. Yao et al, Experimental study on strength and deformation characteristic of normal concrete under triaxial compression. *Build. Sci.* 27(7) (2011) 28-31. (in Chinese)
- [5] P. Launay, H. Gachon, Strain and ultimate strength of concrete under triaxial stresses. Special Publication SP-34, *J. Am. Concr. Inst.* (1) (1970) 269-282.
- [6] YP. Song, Constitutive relation and failure criterion of various concrete materials, first ed., China Water Conserv. and Hydropower Press, Beijing, 2002. (in Chinese)
- [7] Lu Yuan. Mechanical properties of prismatic concrete under uniaxial and triaxial stress [D]. Beijing Jiaotong University, 2017. (in Chinese)
- [8] Chen Yuan. Experimental study on dynamic performance of large aggregate concrete under triaxial compression [D]. Dalian University of Technology, 2013. (in Chinese)
- [9] Ahmad Mahboubi, Ali Ajorloo. Experimental study of the mechanical behavior of plastic concrete in triaxial compression. *Cement and Concrete Research.* (35) (2005) 412-419.
- [10] Nicholas T, Chen S E. Mode I Fatigue of the Carbon fiber-Reinforced Plastic-Concrete Interface Bond. *Experimental Techniques.* (2011).
- [11] Hinchberger S, Weck J, Newson T. Mechanical and hydraulic characterization of plastic concrete forseepage cut-off walls. *J. Canadian Geotechnical.* (2010) 461-471.
- [12] Mahboubi A, Ajorloo A. Experimental study of the mechanical behavior of plastic concrete in triaxial compression. *Cement and Concr. Research.* 35(2) (2005).

- [13] R Detwiler, K Folliard, J Olek et al. Causes and Prevention of Crack development in Plastic Concrete. Portland Cement Association Annual Meeting. (2008) 130-136.
- [14] Morris Peter H, Dux Peter F. Crack depths in desiccating plastic concrete. *ACI Materials J.* (2006) 90-96.
- [15] Sadrekarimi J. Plastic concrete mechanical behaviour. *J. of the Inst. of Eng. (India)*. (2002) 201-207.
- [16] ICOLD. Filling materials for watertight cutoff walls. International Committee of Large Dams: Paris, Bulletin. (1985) (51).
- [17] MJ Deng. Study on the performance of plastic concrete cutoff wall for enclosing dam in East Pinghu. Doc. Diss. Of Tsinghua Univ. (2005).(in Chinese)
- [18] Y Shi, X Chen, JZ Li et al. Study on micro-macroscopic properties of plastic concrete anti-seepage wall with low liquid limit [J/OL]. *Journal of Yangtze River Scientific Research Institute*: 1-7 [2019-03-13]. (in Chinese)
- [19] SQ Song, YJ Chen, Y Han. Experimental study on basic properties of ash-plastic concrete anti-seepage wall material in cement kiln [J]. *Journal of Hydroelectric Engineering*, 2018, 37(07): 58-64. (in Chinese)
- [20] LL Liu, FF Chang, W Xie et al. Analysis of stress-strain curve of plastic concrete under cyclic loading [J]. *Journal of Yangtze River Scientific Research Institute*, 2015, 32 (10): 116-120. (in Chinese)
- [21] China Build. Mater. Sci. Res. Inst. et al, Ordinary Portland cement (GB175-2007). China Stan. Press, Beijing, 2007. (in Chinese)
- [22] China Assoc. of Sand and Gravel et al, Sand for construction (GB/T14684-2011). China Stan. Press, Beijing, 2011. (in Chinese)
- [23] China Three Gorges Corp. et al, Specifications for hydraulic concrete construction (DL/T5144-2001). China Power Press, Beijing, 2002. (in Chinese)